

Received 23 May 2023, accepted 31 May 2023, date of publication 5 June 2023, date of current version 12 July 2023.

Digital Object Identifier 10.1109/ACCESS.2023.3282890

RESEARCH ARTICLE

Detecting Rotational Symmetry in Polar Domain Based on SIFT

HABIB AKBAR^{1,2}, MUHAMMAD MUNWAR IQBAL^{ID 1}, ABID ALI^{ID 1,3}, AMNA PARVEEN^{ID 4},
NAGWAN ABDEL SAMEE^{ID 5}, MANAL ABDULLAH ALOHALI^{ID 6},
AND MOHAMMED SALEH ALI MUTHANNA^{ID 7}

¹Department of Computer Science, University of Engineering and Technology, Taxila, Taxila 47050, Pakistan

²Department of IT, The University of Haripur, Haripur 22620, Pakistan

³Department of Computer Science, GANK(S) DC KTS Haripur, Haripur 22800, Pakistan

⁴College of Pharmacy, Gachon University, Incheon 21936, South Korea

⁵Department of Information Technology, College of Computer and Information Sciences, Princess Nourah bint Abdulrahman University, Riyadh 11671, Saudi Arabia

⁶Department of Information Systems, College of Computer and Information Sciences, Princess Nourah bint Abdulrahman University, Riyadh 11671, Saudi Arabia

⁷Institute of Computer Technologies and Information Security, Southern Federal University, 347922 Taganrog, Russia

Corresponding authors: Manal Abdullah Alohalı (maalohaly@pnu.edu.sa) and Amna Parveen (amnaparvin@gmail.com)

This work was supported by the Princess Nourah bint Abdulrahman University Researchers Supporting Project, Princess Nourah Bint Abdulrahman University, Riyadh, Saudi Arabia, under Grant PNURSP2023R330.

ABSTRACT Symmetry is everywhere, found in objects around us, whether artificial or natural, and acts as a mid-level cue for both human and machine perception of the chaotic real world. From real-world symmetries, humans take advantage of various tasks, but their computational treatment remains elusive. This study proposes a novel approach for detecting rotational symmetry and the order of rotation within a single object digital image. The proposed method relies on the extraction of Scale Invariant Features Transform (SIFT) features and the robust centroid point. The centroid is computed on the basis of extracted features, to be drawn in xy-plan so that the centroid is on the origin. Later on, converted to the polar domain to facilitate the extraction of rotationally symmetric pairs and the order of rotation. The symmetry exhibited by each pair in the transform domain is the function of the features' location, orientation, magnitude, and descriptor vector. Experimental results show that the approach correctly identifies the rotational symmetry if enough features are detected and the centroid is robust one.

INDEX TERMS Symmetry, rotational asymmetry, rotation order, centroid, polar domain, SIFT, detection.

I. INTRODUCTION

Symmetry is everywhere, presenting itself in various forms and scales, from atomic structures to galaxies, and nature to man-made objects. Symmetry is an important visual cue in the perception of the chaotic real world. Humans take advantage of real-world symmetries for various tasks, in machine vision the computational treatment of symmetry remains elusive Funck and Liu [8]. Symmetry not only gives a sense of balance to an appearance but also ties features together that otherwise seem diffuse. Symmetry has a wide range of applications and take the intelligent system to the next

The associate editor coordinating the review of this manuscript and approving it for publication was Amin Zehtabian^{ID}.

level [5], [7], [9], [10], [11], [13], [16], [19], [22], [23], [25], [26], [30], [37], [38].

Perfectly symmetrical objects are rarely found, for approximate symmetries, we must deviate from the ideal condition and assign a continuous value to the degree of symmetry [38]. The mathematical definition of symmetry is clear and straightforward. The symmetry g of a set S is as $g(S) = S$, i.e., the transformation g keeps S invariant as a whole while permuting its parts. In 2D Euclidean geometry, weyl [36], symmetry is of various types, including Reflectional, Rotational, Transnational, and Glide-Reflectional. An object had rotational symmetry of order n if invariant about its center of mass under rotation of $2\pi/n$ radians. Rotational symmetry is further classified into cyclic :(rotation only), dihedral:

(rotation+ reflection), and orthogonal group $O(2)$: (continuous rotation with an infinite number of Reflectional symmetry about the axes through the center of mass) seungkyu et al. [28].

Symmetry attracts people since ancient times and has a long history. A large body is working on the detection of various symmetries dating back to the 1970s. The previous work use either local or global approach to detect symmetry. In global approach, the whole image is treated as a single signal and detect symmetry from that signal via frequency analysis. The work of Marola [24], Keller and Shkolnisky [12], Sun and Si [31] are based on a global approach. The local approach is based on the extraction of local features like edges features, contours, boundary points, corners, and feature points to detect different types of symmetries. The work of Loy and Eklundh [21], Atadjanov and Lee [3], Kawasaki [26], and Lee and Liu [15], Akbar et al. [34] are based on local approach. After Liu et al. [17], some work detects symmetry using deterministic approaches including the work of Atadjanov and Lee [3], Tsogkas and Dickinson [33], Wang et al. [35], and Teo et al. [32]. In recent years, deep learning methods have been applied to symmetry detection. These methods typically rely on convolutional neural networks (CNN's) or recurrent neural networks (RN's) to learn patterns of symmetry in images [1], [8], [6]. Deep learning has indeed demonstrated remarkable success in various computer vision tasks [39], [40], [41], [42], but had limitation when comes to detect symmetry.

The feature based methods detect rotational symmetry without focus on the order of rotation and also using complex voting space that are computationally expensive, sensitive to noise and outliers. The frequency analysis to rotational symmetry detection is highly prone to noise, limited applicability, and computationally intensive. Recently deep learning methods only detect the center of rotation. This study focuses on the detection of planar rotational symmetry and the order of rotation in a single object digital image. The proposed method based on the extraction of SIFT features and drawn in xy-plane so that the center of mass is on the origin. Later on to be converted to polar domain to extract the symmetric pair points w.r.t location, gradient magnitude & direction, and descriptor vector. Each pair poll a single vote for symmetry measure in the transform domain. The symmetric arc is drawn among the matched key points if the number of matches crosses the threshold value $> \rho$.

The contribution of this paper is a novel and effective method to detect rotational symmetry and the order of rotation in single object digital image. The rest of the paper is organized as: section II briefly explains the previous work. The details of the proposed approach discussed in section III. Section IV show the experimental results when applied to real and man-made objects, section V concludes the paper, and section VI discuss the limitations and future work.

II. PREVIOUS WORK

The treatment of different types of symmetries is not only a research topic in computer vision but also in Art, Science, Mathematics, and Architecture. Despite decades of research, the detection of various types of symmetry still remains a challenging task in computer vision and pattern recognition. In 2011, 2013, and 2017 [17], [18], [27], the symmetry detection competitions were held and evaluate state-of-the-art symmetry detection algorithms of their respective time. In these competitions, rotational symmetry has not got much attention and the method of [21] is still used as a baseline.

The existing methods to detect rotational symmetry either used sparse [4], [21], frequency [12], [14], [28] or dense [1], [2], [8] methods. The sparse methods extract features and detect symmetry based on the extracted features, and the frequency analysis used Fourier Transform in the transform domain to detect rotational symmetry. While the dense methods used learning based approaches to detect Rotational symmetry.

A. SPARSE

Loy and Eklundh [21] detect the dominant symmetry present within an image from the symmetric constellations of SIFT [20] features. The symmetry exhibited by each pair is the function of relative location, gradient magnitude & orientation, and the descriptor vector of the corresponding key point in a pair. Later on, the dominant axes/center is detected using Hough voting space. The method can only detect the center of rotation without detecting the rotation order.

In [4], the authors detect the planar rotational symmetry under the affine projection on the basis of various local features including SIFT Lowe [20], Harris-affine, and Hessian-affine features. The rotational symmetry is detected by keeping the best matches and the center of rotation is computed from feature orientations. The proposed method can detect multiple rotational symmetries along with partial occlusion, and supporting region. Prasad and Davis [29] compute the gradient magnitude field encoded in the form of Gradient Vector Flow and construct a graph consist nodes as pixels of the image. The connected nodes are rotationally symmetric and the cycles poll votes for n-cyclic symmetry weighted by GFV and the n-sided polygon.

B. FREQUENCY

Some researchers have used the frequency-based analysis of symmetry including the work of seungkyu et al. [28], lee and Liu [14]. Seungkyu et al. [28] proposed a Frieze-Expansion method by transforming the rotational symmetry into 1D translational symmetry. Discrete Fourier Transform (DFT) is applied to the Frieze-Expansion to detect multiple occurrences of rotational symmetry along with their supporting region in real-world images. In [35], the authors extend the idea of seungkyu et al. [28] and applied to affine skewed rotational symmetry detection adding affine deformation. Keller and Shkolnisky [12] applied the Fast Fourier Transform

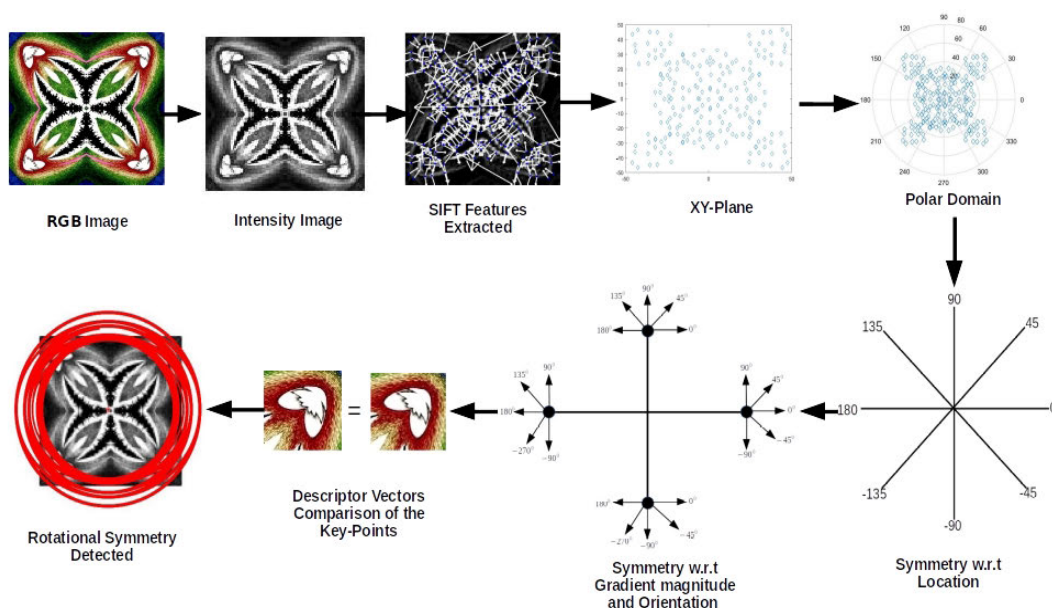


FIGURE 1. Proposed method.

(FFT) in polar coordinates to find signal repetitions over the angular direction to detect rotational symmetry.

C. DENSE

A learning-based approach to rotational and bilateral symmetry detection is proposed by Funck and Liu [8]. For the first time, they applied a multi-layer, fully CNN (called SYMmetry detection neural NETWORK) to detect Reflectional and Rotational symmetry. They trained Sym-NET on MS-COCO data set with ground truths labelled by more than 400 people. The method converts the discrete symmetry into symmetry heat maps and performs well against the existing methods, especially in partially occluded, view-point varied 3D and symmetry at the semantic level. Although CNN’s are known to be shift-invariant, they may not be perfectly invariant to rotation. In other words, if the input image is rotated by some angle, the CNN may not be able to identify the same features as it would in the original image. This can lead to reduced accuracy in detecting rotational symmetry. Seo et al. [1] detects reflectional and rotational symmetry using group equivariant convolutional neural network. Equivariant neural network is able to recognize patterns that are invariant under certain transformations, such as rotations or reflections. To detect rotation symmetry, an equivariant neural network can be trained to identify pairs of points that are rotated versions of each other around a given point. The proposed method leverages the group equivariant features maps of dihedral group of rotation and built dihedrally-equivariant layers that output a spatial map for reflectional axes or rotation center. One potential disadvantage is that group-equivariant neural networks can be sensitive to the choice of symmetry group used. In the case of rotational symmetry detection, for example, different

symmetry groups can be used to represent different types of rotational symmetry, such as 2-fold, 4-fold, or 8-fold symmetry. The choice of symmetry group can have a significant impact on the performance of the neural network, and it may be necessary to experiment with different groups to find the optimal choice for a given task. Both methods claim better performance over the existing algorithms but only finding the rotational center without focusing on detecting the order of rotation. Ponse et al. [2] present another machine learning approach to detects rotational symmetry relies on the reflectional symmetry axis. The proposed method has Limited applicability and inaccurate detection i.e. Not all objects with rotational symmetry have reflectional symmetry and an object may appear to have reflectional symmetry, but in reality, it may have rotational symmetry.

III. PROPOSED METHOD

A. THE PROCEDURE

The RGB image is converted into an intensity/gray scale image that aims to reduce computational complexity. Some preprocessing (like noise removal, gradient image, etc.) is applied before being subjected to SIFT [20] algorithm. Based on the extracted features, the centroid is computed to be placed on the origin of xy-plane. Later on, to be converted to the polar coordinate system, keeping in mind the end goal. The symmetric pairs w.r.t location are extracted by applying the symmetry rules in the polar coordinate system and then comparing the gradient magnitude, orientation, and descriptor vectors of the corresponding key points in a pair to include in the symmetry measure (See Figure.1).

Symmetric pair’s points w.r.t location are extracted using Eqs.(1),(2),(3), and (4). Two threshold values ($T_{\theta} < 0.009$ and $Tr < 5$) are imposed to declare a pair as symmetric w.r.t

Algorithm 1 Symmetry w.r.t Location

Require: SIFT Key Points

Ensure: Symmetric Pairs w.r.t Location

$L = [p_1, p_2, p_3, \dots, p_n]$

for $i \leftarrow 1$ **to** n **do**

for $j \leftarrow 1$ **to** n **do**

$P_i = \frac{d}{2} \cos(\omega\theta_i)$

$P_j = \frac{d}{2} \cos(\omega\theta_j)$

$T_\theta = P_i - P_j$

$T_r = r_i - r_j$

if T_θ and $T_r \approx 0$ **then**

$\chi = P_j$

 Remove P_j from L

end if

end for

end for

location. For more detail, see figures.(2-3).

$$S_i = \frac{d}{2} \cos(\omega\theta_i) \tag{1}$$

$$S_j = \frac{d}{2} \cos(\omega\theta_j) \tag{2}$$

$$T_\theta = S_i - S_j \approx 0 \tag{3}$$

$$T_r = r_i - r_j \approx 0 \tag{4}$$

where r_i, r_j are the distances from the origin, θ_i, θ_j are the angles makes with the polar axis, $\frac{d}{2}$ is the radius means how much far from the origin the points are considered for symmetry measure, and ω is the order of rotation. Once the symmetric pair is extracted w.r.t. location, then the descriptor vectors, gradient magnitudes, and orientations of the corresponding key-points in a pair are compared. The gradient magnitude and orientations are compared by using Eqs. (5), (6), (7), (8), and (9). We set two threshold values (T_ψ, T_m) to measure the symmetry of key points w.r.t gradient magnitude and direction.

$$\alpha = \theta_i - \theta_j \tag{5}$$

$$T_\psi = \psi_i + \alpha - \psi_j \approx 0 \tag{6}$$

$$T_\psi = (\psi_i + \alpha - \psi_j) + 360 \approx 0 \tag{7}$$

$$T_\psi = (\psi_i + \alpha - \psi_j) - 360 \approx 0 \tag{8}$$

$$T_m = M_i - M_j \approx 0 \tag{9}$$

where M_i, M_j are the gradient magnitudes, ψ_i, ψ_j are the gradient orientations, and α is the angle difference between symmetric points w.r.t location. For more detail, see figures.(4-5). Once a pair of points is symmetric w.r.t location, gradient magnitude and orientation, then compare the descriptor vectors of the corresponding key points' to vote for the final symmetry measure. Symmetry exhibited by each pair is the function of relative location, gradient magnitude and direction, and descriptor vectors.

For each ω we impose a threshold value ($T_\omega > 10$) if the number of matched pairs exceeds the threshold value, draw an arc between all the matched points; otherwise not.

Algorithm 2 Gradient Magnitude and Orientation Comparison

Require: Symmetric Pairs w.r.t Location

Ensure: Symmetry Pairs w.r.t Gradient Magnitude and Orientation

$\chi = [m_1, m_2, m_3, \dots, m_n]$

for $i \leftarrow 1$ **to** χ **do**

for $j \leftarrow 1$ **to** χ **do**

$\alpha = \theta_i - \theta_j$

$T_\psi = \psi_i + \alpha - \psi_j$ OR

$T_\psi = \psi_i + \alpha - \psi_j + 360$ OR

$T_\psi = \psi_i + \alpha - \psi_j - 360$

$T_m = M_i - M_j$

if T_ψ and $T_m \approx 0$ **then**

$\chi = m_j$

end if

end for

end for

Algorithm 3 Descriptor Vector Comparison

Require: Symmetric Pairs w.r.t Location, Gradient Magnitude and Orientation

Ensure: Symmetric Pairs w.r.t Descriptor Vectors

$\chi = [m_1, m_2, m_3, \dots, m_n]$

for $i \leftarrow 1$ **to** χ **do**

for $j \leftarrow 1$ **to** χ **do**

if $D_i == T_j$ **then**

$\chi = m_j$

end if

end for

end for

Algorithm 4 Rotational Symmetry Detection

Require: SIFT Key Points

Ensure: Rotational Symmetry detection

$\chi = [m_1, m_2, m_3, \dots, m_n]$

if T_θ and $T_r \approx 0$ **then** Algorithm 1

if T_ψ and $T_m \approx 0$ **then** Algorithm 2

if $D_i \approx D_j$ **then** Algorithm 3

if $m_i \geq T_\omega$ **than**

 Draw an Arc

 among all Points in m_i

end if

end if

end if

B. EXAMPLE ILLUSTRATION

Let p_i, p_j be any two points with $r_i = 5, r_j = 5$ and $\theta_i = 0, \theta_j = 45$, putting the values in Eqs. (1), (2), (3), and (4) to calculate T_r and T_θ .

$$T_r = 5 - 5 = 0$$

The threshold T_r Satisfy the condition, i.e., either zero or nearly to zero.

Now for threshold T_θ , the following calculation is required:

For $\omega = 1$
 $S_i = \cos(1 \times 0) = 1$
 $S_j = \cos(1 \times 45) = 0.707$
 $T_\theta = (1 - 0.707) \neq 0$
 For $\omega = 2$
 $S_i = \cos(2 \times 0) = 1$
 $S_j = \cos(2 \times 45) = 0$
 $T_\theta = (1 - 0) \neq 0$
 For $\omega = 3$
 $S_i = \cos(3 \times 0) = 1$
 $S_j = \cos(3 \times 45) = (-0.707)$
 $T_\theta = (1 - (-0.707)) \neq 0$
 For $\omega = 4$
 $S_i = \cos(4 \times 0) = 1$
 $S_j = \cos(4 \times 45) = -1$
 $T_\theta = (1 - (-1)) \neq 0$
 For $\omega = 5$
 $S_i = \cos(5 \times 0) = 1$

$S_j = \cos(5 \times 45) = -0.707$
 $T_\theta = 1 - (-0.707) \neq 0$
 For $\omega = 6$
 $S_i = \cos(6 \times 0) = 1$
 $S_j = \cos(6 \times 45) = 0$
 $T_\theta = 1 - 0 \neq 0$
 For $\omega = 7$
 $S_i = \cos(7 \times 0) = 1$
 $S_j = \cos(7 \times 45) = 0.707$
 $T_\theta = 1 - 0.707 \neq 0$
 And For $\omega = 8$
 $S_i = \cos(8 \times 0) = 1$
 $S_j = \cos(8 \times 45) = 1$
 $T_\theta = 1 - 1 = 0$

So the threshold T_θ is satisfied for $\omega=8$. Hence the above points are rotationally symmetric w.r.t location with rotation order 8. Similarly, for other symmetric pair points w.r.t location, Eqs. (1), (2), (3), and (4) are used to extract the

$$T_\Psi = \Psi_i + \alpha - \Psi_j \left\{ \begin{array}{l} \forall [\theta_i, \theta_j \geq 0], \quad \left\{ \begin{array}{l} \{\Psi_i, \Psi_j > 0\}, \quad (\theta_i > \theta_j \parallel \theta_i < \theta_j, \Psi_i > \Psi_j \parallel \Psi_i < \Psi_j) \\ \{\Psi_i, \Psi_j < 0\}, \quad (\theta_i > \theta_j \parallel \theta_i < \theta_j, \Psi_i > \Psi_j \parallel \Psi_i < \Psi_j) \\ \{\Psi_i > 0, \Psi_j < 0\}, \quad (\theta_i > \theta_j, \Psi_i > \Psi_j) \\ \{\Psi_i < 0, \Psi_j > 0\}, \quad (\theta_i < \theta_j, \Psi_i < \Psi_j) \end{array} \right. \\ \\ \forall [\theta_i > 0, \theta_j < 0], \quad \left\{ \begin{array}{l} \{\Psi_i, \Psi_j > 0\}, \quad (\theta_i < \theta_j, \Psi_i < \Psi_j) \\ \{\Psi_i, \Psi_j < 0\}, \quad (\theta_i < \theta_j, \Psi_i < \Psi_j) \\ \{\Psi_i < 0, \Psi_j > 0\}, \quad (\theta_i < \theta_j, \Psi_i < \Psi_j) \end{array} \right. \\ \\ \forall [\theta_i < 0, \theta_j > 0], \quad \left\{ \begin{array}{l} \{\Psi_i, \Psi_j > 0\}, \quad (\theta_i > \theta_j, \Psi_i > \Psi_j) \\ \{\Psi_i, \Psi_j < 0\}, \quad (\theta_i > \theta_j, \Psi_i > \Psi_j) \\ \{\Psi_i > 0, \Psi_j < 0\}, \quad (\theta_i > \theta_j, \Psi_i > \Psi_j) \end{array} \right. \\ \\ \forall [\theta_i, \theta_j < 0], \quad \left\{ \begin{array}{l} \{\Psi_i, \Psi_j > 0\}, \quad (\theta_i > \theta_j \parallel \theta_i < \theta_j, \Psi_i > \Psi_j \parallel \Psi_i < \Psi_j) \\ \{\Psi_i, \Psi_j < 0\}, \quad (\theta_i > \theta_j, \Psi_i > \Psi_j) \\ \{\Psi_i > 0, \Psi_j < 0\}, \quad (\theta_i < \theta_j, \Psi_i < \Psi_j) \\ \{\Psi_i < 0, \Psi_j > 0\}, \quad (\theta_i < \theta_j, \Psi_i < \Psi_j) \end{array} \right. \end{array} \right.$$

$$T_\Psi = (\Psi_i + \alpha - \Psi_j) + 360 \left\{ \begin{array}{l} \forall [\theta_i < 0, \theta_j > 0] \quad \left\{ \begin{array}{l} \{\Psi_i, \Psi_j > 0\}, \quad (\theta_i > \theta_j, \Psi_i < \Psi_j) \\ \{\Psi_i, \Psi_j < 0\}, \quad (\theta_i > \theta_j, \Psi_i < \Psi_j) \\ \{\Psi_i < 0, \Psi_j > 0\}, \quad (\theta_i > \theta_j, \Psi_i < \Psi_j) \end{array} \right. \\ \\ \forall [\theta_i, \theta_j > 0] \quad \left\{ \begin{array}{l} \{\Psi_i < 0, \Psi_j > 0\}, \quad (\theta_i > \theta_j, \Psi_i < \Psi_j) \\ \{\Psi_i < 0, \Psi_j < 0\}, \quad (\theta_i > \theta_j, \Psi_i < \Psi_j) \end{array} \right. \\ \\ \forall [\theta_i, \theta_j < 0] \quad \left\{ \begin{array}{l} \{\Psi_i < 0, \Psi_j < 0\}, \quad (\theta_i > \theta_j, \Psi_i < \Psi_j) \end{array} \right. \end{array} \right.$$

$$T_\Psi = (\Psi_i + \alpha - \Psi_j) - 3600 \left\{ \begin{array}{l} \forall [\theta_i > 0, \theta_j < 0] \quad \left\{ \begin{array}{l} \{\Psi_i, \Psi_j > 0\}, \quad (\theta_i < \theta_j, \Psi_i > \Psi_j) \\ \{\Psi_i, \Psi_j < 0\}, \quad (\theta_i < \theta_j, \Psi_i > \Psi_j) \\ \{\Psi_i > 0, \Psi_j < 0\}, \quad (\theta_i < \theta_j, \Psi_i > \Psi_j) \end{array} \right. \\ \\ \forall [\theta_i, \theta_j > 0] \quad \left\{ \begin{array}{l} \{\Psi_i > 0, \Psi_j < 0\}, \quad (\theta_i < \theta_j, \Psi_i < \Psi_j) \\ \{\Psi_i > 0, \Psi_j < 0\}, \quad (\theta_i < \theta_j, \Psi_i < \Psi_j) \end{array} \right. \\ \\ \forall [\theta_i, \theta_j < 0] \quad \left\{ \begin{array}{l} \{\Psi_i > 0, \Psi_j < 0\}, \quad (\theta_i < \theta_j, \Psi_i > \Psi_j) \end{array} \right. \end{array} \right.$$

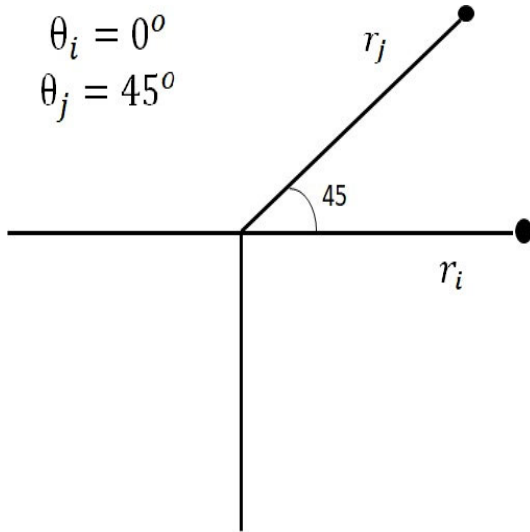


FIGURE 2. Symmetric points w.r.t location with $r_i=5, r_j=5$ and $\theta_i=0, \theta_j=45$.

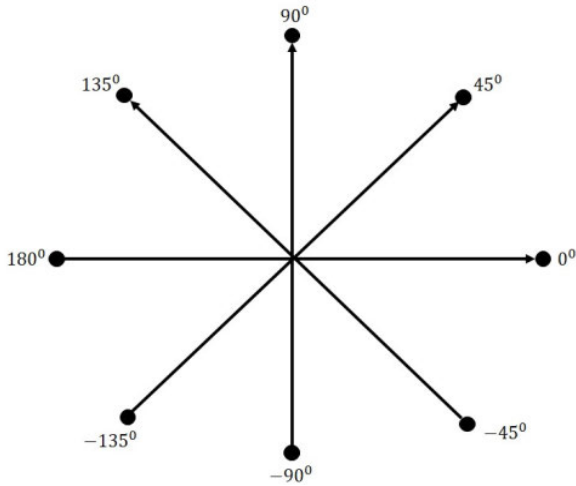


FIGURE 3. Symmetric points w.r.t location.

symmetric pairs. Figures.(2-3) show that if a point p_i is on the polar axis and p_j forms 45 degrees With a polar axis, then the two points are symmetric with rotational order of $\omega=8$ and so on.

Once the symmetric pairs points are extracted, then the symmetry of gradient magnitude and orientation is computed using Eqs. (5), (6), (7), (8), and (9). From Figure.4, it is clear that if a point p_i having gradient orientation ($\psi = 45$) then their corresponding symmetric points p_j for $j=2, 3, 4$ will have $\psi_j=45,135,135$.

Let P_i having $\psi_j = 45$ and $M_i = 6, \theta_i = 0$, and P_j having $\psi_j = (0,45,90,135,180,45,90,135), M_j = 6, \theta_j = 90$.

Since $\psi_i, \psi_j > 0$ and $\theta_i, \theta_j > 0$, Using Eqs. (5), (6), and (9) to calculate the values of T_ψ, T_m , and α .

$$\alpha = \theta_i - \theta_j$$

$$\text{So } \alpha = 90 - 0 = 90$$

$$T_m = M_i - M_j$$

$$\text{so } T_m = 6 - 6 = 0$$

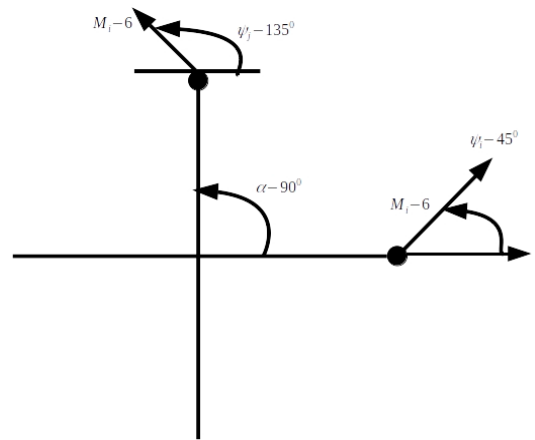


FIGURE 4. Symmetric pair points w.r.t gradient magnitude and orientation with P_i having $\psi_i=45, M_i=6, \theta_i=0$, and P_j having $\psi_j=135, M_j=6, \theta_j=90$.

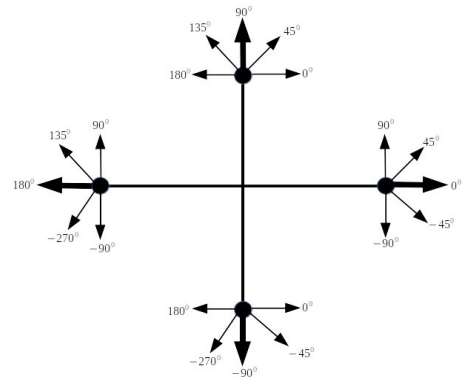


FIGURE 5. Symmetry w.r.t Gradient Magnitude and Orientation where P_i having $\psi_i=0, M_i=6$, and $\theta_i=0$, the corresponding symmetric point P_j having $\psi_j=90, \psi_j=180, \psi_j=-90, M_j=6, \theta_j=90/\omega=4$.

Now for $\psi_j = 0$

$$T_\psi = 45 + 90 - 0 = 135$$

For $\psi_j = 45$

$$T_\psi = 45 + 90 - 45 = 90$$

For $\psi_j = 90$

$$T_\psi = 45 + 90 - 90 = 45$$

For $\psi_j = 135$

$$T_\psi = 45 + 90 - 135 = 0$$

For $\psi_j = 180$

$$T_\psi = 45 + 90 - 180 = -45$$

For $\psi_j = -45$

$$T_\psi = 45 + 90 + 45 = 180$$

For $\psi_j = -90$

$$T_\psi = 45 + 90 + 90 = 225$$

For $\psi_j = -135$

$$T_\psi = 45 + 90 + 135 = 270$$

From the above calculation, the value of T_ψ at $\psi_j=135$ satisfy the condition. So P_i, P_j are symmetric for $\psi_i=45, M_i=6, \theta_i=0$ and $\psi_j=135, M_j=6, \theta_j=90$.

Figures.(5-6-7-8) show the symmetry of gradient magnitude and orientation of key point P_i having $\psi_i=0,45,90,180$

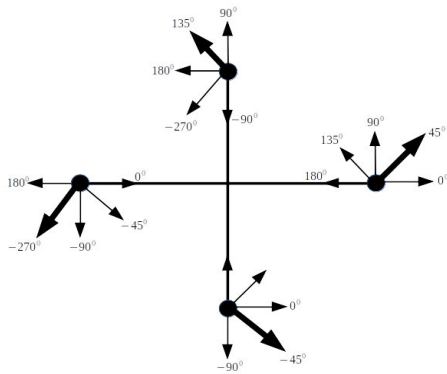


FIGURE 6. Symmetry w.r.t Gradient Magnitude and Orientation where P_i having $\psi_i=45$, $M_i=6$, and $\theta_i=45$, the corresponding symmetric point P_j having $\psi_j=135$, $\psi_j=-135$, $\psi_j=-45$, $M_j=6$, $\theta_j=90/\omega=4$.

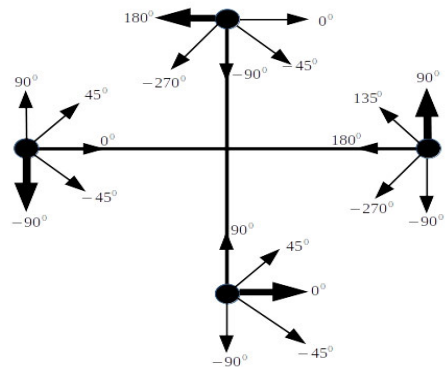


FIGURE 7. Symmetry w.r.t Gradient Magnitude and Orientation where P_i having $\psi_i=90$, $M_i=6$, and $\theta_i=90$, the corresponding symmetric point P_j having $\psi_j=180$, $\psi_j=-90$, $\psi_j=0$, $M_j=6$, $\theta_j=90/\omega=4$.

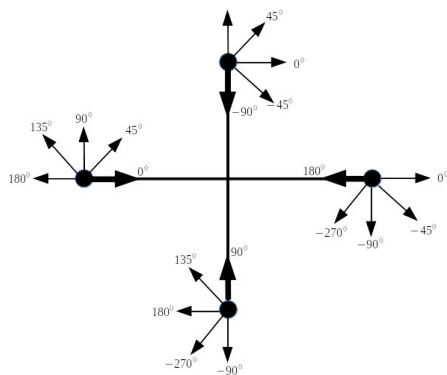


FIGURE 8. Symmetry w.r.t Gradient Magnitude and Orientation where P_i having $\psi_i=180$, $M_i=6$, and $\theta_i=180$, the corresponding symmetric point P_j having $\psi_j=90$, $\psi_j=0$, $\psi_j=90$, $M_j=6$, $\theta_j=90/\omega=4$.

and their corresponding symmetric point P_j having $\psi_j=90, 180, -90, \psi_j=135, -135, -45, \psi_j=180, -90, 90$ and $\psi_j=-90, 0, 90$ with rotational order $\omega=4$.

IV. RESULTS

The experimental results of the proposed method are based on confusion matrix. True positive means the symmetry reported

in symmetric objects and False negative means Asymmetry reported in symmetric objects. False positive means the symmetry reported in Asymmetric objects, while a True negative means the asymmetry reported in asymmetric objects.

Performance of the proposed method is measured using Accuracy, Precision, recall, and a single-valued score called F-Measure. The Precision, recall, and F-Score is calculated as the following:

$Precision = TP/(TP + FP)$ Precision is the measure of correct detection among all those detection's that the algorithm believes are true one. Precision measure exactness of the algorithm.

$$Recall = TP/(TP + FN)$$

Recall is the measure of correct detection, i.e. true positive detection among all symmetric objects. Recall measuring the completeness of the algorithm.

Note that TP, FP, FN means True Positive, False Positive, and False Negative.

$$F - Score = 2 \times P \times R / P + R$$

The proposed method is tested on a dataset of 200 images collected from various sources on the internet. Out of 200 images, 170 are rotationally symmetric, and 30 are Asymmetric. Out of 170, 100 were synthetic, and 70 were real-world images, of which some photos have background clutter. The approach identifies rotational symmetry in 165 out of 200, of which 155 are identified correctly while 10 are identified incorrectly. For Asymmetric images, the method identifies 25 out of 30 as Asymmetric. Figure.7 show the true results of the proposed method on the experimental dataset. To measure the performance of the proposed method, we compute Precision, Recall, F-Score. The precision, recall, and F-Score based on the above information is calculated as follows:

$$Precision=155/165=0.93$$

$$Recall=155/170=0.91$$

$$F\text{-score}=0.91$$

From the above calculation, the approach reported 0.93 Precision, 0.91 recall, 0.91 F-Score. Table.1 show the performance of the proposed approach on the experimental dataset. It is evident from Table.1 that the proposed method reported 93.0% True Positive rate and 07.0% False Positive rate. Here True Positive means the correct detection of symmetry in symmetric objects and False Positive means detect symmetry in asymmetric objects. Similarly the True Negative rate is 95.0% and the False Negative is 5.0%. True negative means asymmetry reported in asymmetric objects and False negative means symmetry reported in asymmetric objects.

Table.2 show the True Positive and False Positive rate of the proposed method for synthetic and natural objects. The true positive rate for the synthetic images is superior because of a high degree of symmetry present in such types of objects. We also compute the accuracy of the proposed method as shown in Table.3. Accuracy measure the overall performance of the proposed method.

Table.4 show the comparison of the proposed method with Loy and Eklundh [21] in term of F-Score. The detection rate

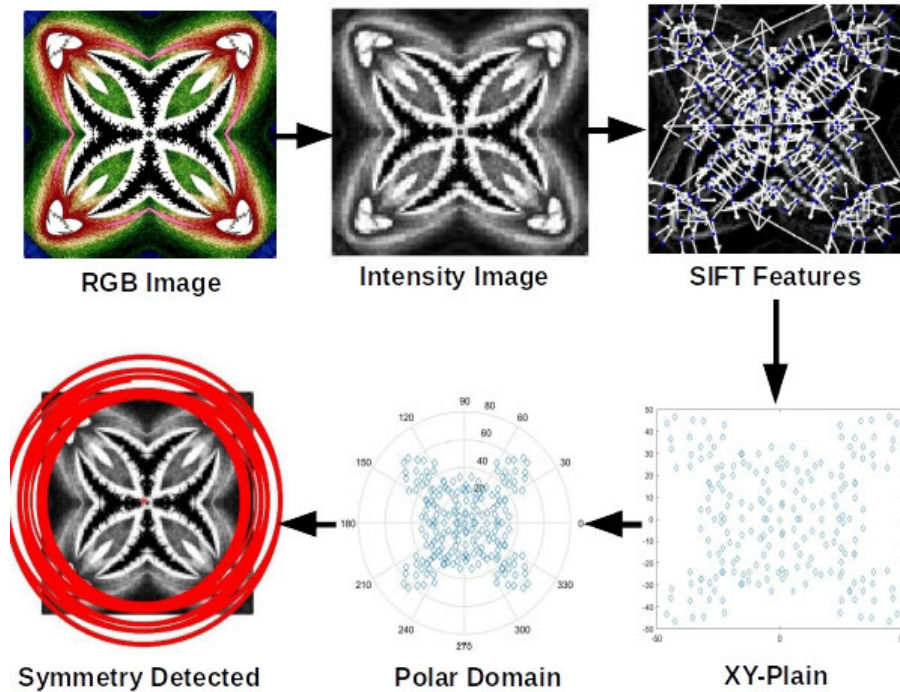


FIGURE 9. Symmetry detection example illustration.

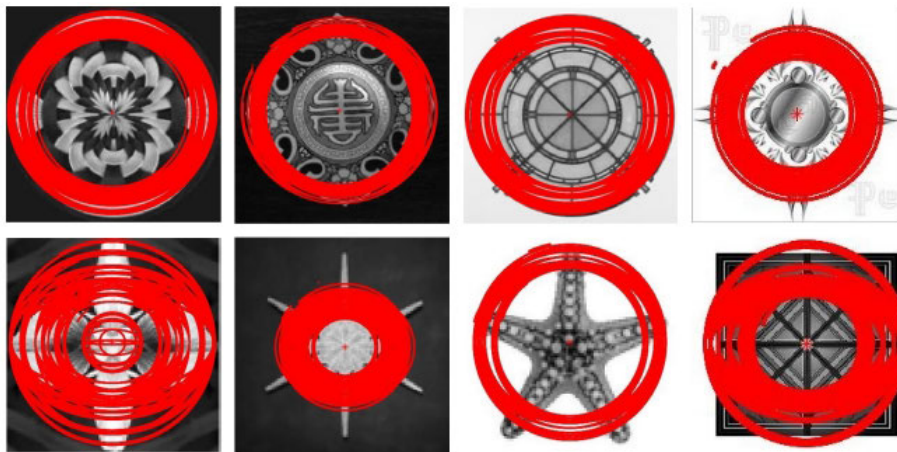


FIGURE 10. Results of the proposed method on experimental dataset.

TABLE 1. Results of the our method on experimental dataset.

Test Outcome	True Positive	False Positive
Symmetric	91.0%	09.0%
Asymmetric	17.0%	83.0%
	False Negative	True Negative

of the proposed method is superior to Loy and Eklundh [21] in the case of images with no background clutter, while inferior for images having strong background clutter.

Table.5 show the qualitative comparison of the proposed method with Funck and Liu [8] and Seo et al. [1]. The proposed method is able to detect rotational symmetry, center of rotation, order of rotation and failed to detects multiple

TABLE 2. Results of the proposed method for real and synthetic images.

Test Outcome	True Positive	False Positive
Synthetic	91.5%	08.5%
Natural	87.67%	12.33%

TABLE 3. Accuracy of the proposed method for real and synthetic images.

Test Outcome	Synthetic	Natural	Combined
Accuracy	82.1%	85.7%	87.0%

occurrences of rotational symmetry. The methods of Funck and Liu [8] and Seo et al. [1] only detects the multiple centers rotation.

TABLE 4. Comparison of our approach with loy [21].

Test Outcome	Our Approach	Loy
Image Without Background Clutter	.91	.85
Image With Background Clutter	.60	.83

TABLE 5. Comparison of Our Approach with Funck [8], Seo [1].

Test Outcome	Our	[1]	[2]
Rot. Symmetry	yes	yes	yes
Rot. Center	yes	yes	yes
Rot. Order	yes	No	No
Rot. Multiple	No	yes	yes

V. CONCLUSION

The study investigate a novel and effective method to detect rotational symmetry within a single object digital image. The proposed method relies on the extraction of SIFT features that serve as a basis for computing the centroid of the object to be drawn in the Cartesian Coordinate system. Later on, to be converted into polar coordinate system to facilitate the extraction of rotationally symmetric pairs points. The symmetric pair points w.r.t location is extracted based on symmetry rules defined in Eqs.(1),(2),(3), and (4) in the polar coordinate system. This is followed by comparing the descriptor vectors, gradient magnitude, and orientation of the corresponding key points in a pair using Eqs.(5),(6),(7),(8), and (9) to include the pair in the final symmetry measure. The proposed method successfully detect the rotational symmetry and the order of rotation in single object digital image. The proposed method relies on the robust extraction of SIFT features and computed centroid points. The experimental results are satisfactory if enough features are extracted and the centroid is a robust one.

VI. LIMITATIONS AND FUTURE WORK

The performance of the proposed method is unsatisfactory for images with strong background clutter and unable to detects multiple occurrences of rotational symmetry.

Deep learning has shown remarkable success in a wide range of computer vision tasks. However, there are some limitations of deep learning when it comes to detecting rotational symmetry i.e. rotational invariance and particularly limitations of the training data.

In future, we need to carefully consider these limitations and work to develop techniques that can address them to improve the effectiveness in detecting rotational symmetry.

REFERENCES

- [1] A. Seo, B. Kim, S. Kwak, and M. Cho, "Reflection and rotation symmetry detection via equivariant learning," in *Proc. IEEE/CVF Conf. Comput. Vis. Pattern Recognit. (CVPR)*, Jun. 2022, pp. 9529–9538.
- [2] K. Ponse, A. V. Kononova, M. Loley, and B. Van Stein, "Using machine learning to detect rotational symmetries from reflectional symmetries in 2D images," in *Proc. IEEE Symp. Ser. Comput. Intell. (SSCI)*, Dec. 2021, pp. 01–08.
- [3] I. Atadjanov and S. Lee, "Bilateral symmetry detection based on scale invariant structure feature," in *Proc. IEEE Int. Conf. Image Process. (ICIP)*, Sep. 2015, pp. 3447–3451.
- [4] H. Cornelius and G. Loy, "Detecting rotational symmetry under affine projection," in *Proc. 18th Int. Conf. Pattern Recognit. (ICPR)*, vol. 2, 2006, pp. 292–295.
- [5] A. Dai, A. X. Chang, M. Savva, M. Halber, T. Funkhouser, and M. Nießner, "ScanNet: Richly-annotated 3D reconstructions of indoor scenes," in *Proc. IEEE Conf. Comput. Vis. Pattern Recognit. (CVPR)*, Jul. 2017, pp. 2432–2443.
- [6] S. Sundaram, D. Sinha, M. Groth, T. Sasaki, and X. Boix, "Recurrent connections facilitate symmetry perception in deep networks," *Sci. Rep.*, vol. 12, no. 1, p. 20931, Dec. 2022.
- [7] H. Fan, H. Su, and L. Guibas, "A point set generation network for 3D object reconstruction from a single image," in *Proc. IEEE Conf. Comput. Vis. Pattern Recognit. (CVPR)*, Jul. 2017, pp. 2463–2471.
- [8] C. Funk and Y. Liu, "Beyond planar symmetry: Modeling human perception of reflection and rotation symmetries in the wild," in *Proc. IEEE Int. Conf. Comput. Vis. (ICCV)*, Oct. 2017, pp. 793–803.
- [9] C. Funk and Y. Liu, "Symmetry reCAPTCHA," in *Proc. IEEE Conf. Comput. Vis. Pattern Recognit. (CVPR)*, Jun. 2016, pp. 5165–5174.
- [10] D. C. Hauage and N. Snavely, "Image matching using local symmetry features," in *Proc. IEEE Conf. Comput. Vis. Pattern Recognit.*, Jun. 2012, pp. 206–213.
- [11] W. Hong, A. Y. Yang, K. Huang, and Y. Ma, "On symmetry and multiple-view geometry: Structure, pose, and calibration from a single image," *Int. J. Comput. Vis.*, vol. 60, no. 3, pp. 241–265, Dec. 2004.
- [12] Y. Keller and Y. Shkolnisky, "A signal processing approach to symmetry detection," *IEEE Trans. Image Process.*, vol. 15, no. 8, pp. 2198–2207, Aug. 2006.
- [13] A. Kuehnlé, "Symmetry-based recognition of vehicle rears," *Pattern Recognit. Lett.*, vol. 12, no. 4, pp. 249–258, Apr. 1991.
- [14] S. Lee and Y. Liu, "Skewed rotation symmetry group detection," *IEEE Trans. Pattern Anal. Mach. Intell.*, vol. 32, no. 9, pp. 1659–1672, Sep. 2010.
- [15] S. Lee and Y. Liu, "Curved glide-reflection symmetry detection," *IEEE Trans. Pattern Anal. Mach. Intell.*, vol. 34, no. 2, pp. 266–278, Feb. 2012.
- [16] J. Liu, J. Mundy, and A. Zisserman, "Grouping and structure recovery for images of objects with finite rotational symmetry," in *Proc. Asian Conf. Comput. Vis.*, vol. 1, 1995, pp. 379–382.
- [17] J. Liu, G. Slota, G. Zheng, Z. Wu, M. Park, S. Lee, I. Rauschert, and Y. Liu, "Symmetry detection from RealWorld images competition 2013: Summary and results," in *Proc. IEEE Conf. Comput. Vis. Pattern Recognit. Workshops*, Jun. 2013, pp. 200–205.
- [18] C. Funk, S. Lee, M. R. Oswald, S. Tsogkas, W. Shen, A. Cohen, S. Dickinson, and Y. Liu, "2017 ICCV challenge: Detecting symmetry in the wild," in *Proc. IEEE Int. Conf. Comput. Vis. Workshops (ICCVW)*, Oct. 2017, pp. 1692–1701.
- [19] G. Li, Y. Xie, L. Lin, and Y. Yu, "Instance-level salient object segmentation," in *Proc. IEEE Conf. Comput. Vis. Pattern Recognit. (CVPR)*, Jul. 2017, pp. 247–256.
- [20] D. G. Lowe, "Distinctive image features from scale-invariant keypoints," *Int. J. Comput. Vis.*, vol. 60, no. 2, pp. 91–110, Nov. 2004.
- [21] G. Loy and J.-O. Eklundh, "Detecting symmetry and symmetric constellations of features," in *Proc. Eur. Conf. Comput. Vis.* Cham, Switzerland: Springer, 2006, pp. 508–521.
- [22] M. Lukáč, D. Sýkora, K. Sunkavalli, E. Shechtman, O. Jamriška, N. Carr, and T. Pajdla, "Nautilus: Recovering regional symmetry transformations for image editing," *ACM Trans. Graph.*, vol. 36, no. 4, pp. 1–11, Aug. 2017.
- [23] M. Mancas, B. Gosselin, and B. Macq, "Fast and automatic tumoral area localisation using symmetry," in *Proc. IEEE Int. Conf. Acoust., Speech, Signal Process.*, Sep. 2005, p. 725.
- [24] G. Marola, "On the detection of the axes of symmetry of symmetric and almost symmetric planar images," *IEEE Trans. Pattern Anal. Mach. Intell.*, vol. 11, no. 1, pp. 104–108, 1989.
- [25] J. Pritts, O. Chum, and J. Matas, "Rectification, and segmentation of coplanar repeated patterns," in *Proc. IEEE Conf. Comput. Vis. Pattern Recognit.*, Jun. 2014, pp. 2973–2980.
- [26] N. Kawasaki, "Parametric study of thermal and chemical nonequilibrium nozzle flow," M.S. thesis, Dept. Electron. Eng., Osaka Univ., Osaka, Japan, 1993.
- [27] I. Rauschert, J. Liu, K. Brockelhurst, S. Kashyap, and Y. Liu, "Symmetry detection competition: A summary of how the competition is carried out," in *Proc. IEEE CVPR Workshop Symmetry Detection Real World Images*, Sep. 2011, pp. 1–66.

- [28] L. Seungkyu, R. Collins, and L. Yanxi, "Rotation symmetry group detection via frequency analysis of frieze-expansions," Dept. Comput. Sci. Eng., The Pennsylvania State Univ., Pennsylvania, PA, USA, Tech. Rep. 978-1-4244-2243-2/08, 2008.
- [29] V. Shiv Naga Prasad and L. S. Davis, "Detecting rotational symmetries," in *Proc. 10th IEEE Int. Conf. Comput. Vis. (ICCV)*, vol. 1, Jun. 2005, pp. 954–961.
- [30] P. Speciale, M. R. Oswald, A. Cohen, and M. Pollefeys, "A symmetry prior for convex variational 3D reconstruction," in *Proc. Eur. Conf. Comput. Vis.* Cham, Switzerland: Springer, 2016, pp. 313–328.
- [31] C. Sun and D. Si, "Fast reflectional symmetry detection using orientation histograms," *Real-Time Imag.*, vol. 5, no. 1, pp. 63–74, Feb. 1999.
- [32] C. L. Teo, C. Fermüller, and Y. Aloimonos, "Detection and segmentation of 2D curved reflection symmetric structures," in *Proc. IEEE Int. Conf. Comput. Vis. (ICCV)*, Dec. 2015, pp. 1644–1652.
- [33] S. Tsogkas and S. Dickinson, "AMAT: Medial axis transform for natural images," in *Proc. IEEE Int. Conf. Comput. Vis. (ICCV)*, Oct. 2017, pp. 2727–2736.
- [34] H. Akbar, K. Hayat, N. U. Haq, and U. I. Bajwa, "Bilateral symmetry detection on the basis of scale invariant feature transform," *PLoS ONE*, vol. 9, no. 8, Aug. 2014, Art. no. e103561.
- [35] Z. Wang, Z. Tang, and X. Zhang, "Reflection symmetry detection using locally affine invariant edge correspondence," *IEEE Trans. Image Process.*, vol. 24, no. 4, pp. 1297–1301, Apr. 2015.
- [36] H. Weyl, *Symmetry*, vol. 46. Princeton, NJ, USA: Princeton Univ. Press, 1952, p. 4.
- [37] H. Zabrodsky, S. Peleg, and D. Avnir, "Completion of occluded shapes using symmetry," in *Proc. IEEE Conf. Comput. Vis. Pattern Recognit.*, Jun. 1993, pp. 678–679.
- [38] H. Zabrodsky, S. Peleg, and D. Avnir, "Symmetry as a continuous feature," *IEEE Trans. Pattern Anal. Mach. Intell.*, vol. 17, no. 12, pp. 1154–1166, 1995.
- [39] J. Zhang, Y. Li, W. Xiao, and Z. Zhang, "Non-iterative and fast deep learning: Multilayer extreme learning machines," *J. Franklin Inst.*, vol. 357, no. 13, pp. 8925–8955, Sep. 2020.
- [40] J. Zhang, Y. Zhao, F. Shone, Z. Li, A. F. Frangi, S. Q. Xie, and Z.-Q. Zhang, "Physics-informed deep learning for musculoskeletal modeling: Predicting muscle forces and joint kinematics from surface EMG," *IEEE Trans. Neural Syst. Rehabil. Eng.*, vol. 31, pp. 484–493, 2023.
- [41] A. Kirillov, E. Mintun, N. Ravi, H. Mao, C. Rolland, L. Gustafson, T. Xiao, S. Whitehead, A. C. Berg, W.-Y. Lo, P. Dollár, and R. Girshick, "Segment anything," 2023, *arXiv:2304.02643*.
- [42] S. S. A. Zaidi, M. S. Ansari, A. Aslam, N. Kanwal, M. Asghar, and B. Lee, "A survey of modern deep learning based object detection models," *Digit. Signal Process.*, vol. 126, Jun. 2022, Art. no. 103514.



data, task scheduling, data mining, cloud, mobile cloud computing, and ICN.



Department of Computer Science, University of Engineering and Technology, Taxila, Pakistan. He has authored or coauthored journals and conference papers at the national and international level in the field of computer science. His research interests include machine learning, databases, semantics web, eLearning, and artificial intelligence.



machine learning, data mining, cloud and mobile cloud computing, and ICN.



with the College of Pharmacy, Gachon University, South Korea, where she has been an Assistant Professor, since 2016. She is an expert in the field of natural product chemistry, particularly for the discovery of bioactive constituents from medicinal plants against pharmacological conditions. She has published several research articles in different national and international journals. Her research interests include isolation and identification of potential new constituents from traditionally used medicinal plants that may have potential against various pharmacological conditions such as cancer, diabetes, aging, and neurodegenerative diseases. She has an ongoing interest in identification of bioactive constituents from natural resources for aging and life span extension.



include data science, machine learning, bioinformatics, and parallel computing. Her awards and honors include the Takaful Prize (Innovation Project Track), the Princess Nourah Award in innovation, the Mastery Award in predictive analytics (IBM), the Mastery Award in big data (IBM), and the Mastery Award in cloud computing(IBM).

MANAL ABDULLAH ALOHALI received the Ph.D. degree in computer science from the University of Plymouth, U.K. She is currently an Assistant Professor with the Information Systems Department, CCIS, Princess Nourah bint Abdulrahman University (PNU), Saudi Arabia. She is also the Dean of CCIS. Her research interests include information systems, machine learning, and cyber security. She received the PNU Research Excellence Award.



mobile edge computing, software-defined networks (SDN), the IoT, and industrial wireless and sensor networks.

...